PHYSICAL REVIEW B **85**, 140503(R) (2012)

# Quantum speeding-up of computation demonstrated in a superconducting two-qubit processor

Andreas Dewes,[1] Romain Lauro,[1] Florian R. Ong,[1] Vivient Schmitt,[1] Perola Milman,[2,3] Patrice Bertet,[1] Denis Vion,[1] and Daniel Esteve[1]

[1]*Service de Physique de l'Etat Condensé/IRAMIS/DSM (CNRS URA 2464), CEA Saclay, 91191 Gif-sur-Yvette, France*

[2]*Laboratoire Matériaux et Phénomènes Quantiques, Université Paris Diderot, 10 rue Alice Domon et Léonie Duquet, 75205 Paris, France*

[3]*Université Paris-Sud 11, Institut de Sciences Moléculaires d'Orsay (CNRS), 91405 Orsay, France*

(Received 20 October 2011; revised manuscript received 31 January 2012; published 5 April 2012)

We operate a superconducting quantum processor consisting of two tunable transmon qubits coupled by a swapping interaction, and equipped with nondestructive single-shot readout of the two qubits. With this processor, we run the Grover search algorithm among four objects and find that the correct answer is retrieved after a single run with a success probability between 0.52 and 0.67, which is significantly larger than the 0.25 achieved with a classical algorithm. This constitutes a proof of concept for the quantum speed-up of electrical quantum processors.

DOI: 10.1103/PhysRevB.85.140503 PACS number(s): 85.25.Cp, 03.67.Lx, 74.78.Na

The proposition of quantum algorithms[1–3] that perform useful computational tasks more efficiently than classical algorithms has motivated the realization of physical systems[4] able to implement them and to demonstrate quantum speed-up. The versatility and the potential scalability of electrical circuits make them very appealing for implementing a quantum processor built as sketched in Fig. 1. Ideally, a quantum processor consists of a scalable set of quantum bits that can be efficiently reset, that can follow any unitary evolution needed by an algorithm using a universal set of single- and two-qubit gates, and that can be read projectively.[5] The nonunitary projective readout operations can be performed at various stages of an algorithm, and in any case at the end in order to get the final outcome. Quantum processors based on superconducting qubits have already been operated, but they fail to meet the above criteria in different aspects. With the transmon qubit[6,7] derived from the Cooper pair box,[8] simple quantum algorithms, namely, the Deutsch-Jozsa algorithm,[9] the Grover search algorithm,[1] and a three-qubit quantum error correction code, were demonstrated in two- and three-qubit processors with the coupling between the qubits mediated by a cavity also used for readout.[10,11] In this circuit, the qubits are not read independently, but the value of a single collective variable is determined from the cavity transmission measured over a large number of repeated sequences. By applying suitable qubit rotations prior to this measurement, the density matrix of the two-qubit register was inferred at different steps of the algorithm, and it was found to be in good agreement with the predicted one. Demonstrating quantum speed-up is, however, more demanding than measuring a collective qubit variable since it requests to obtain an outcome after a single run, i.e., to perform the single-shot readout of the qubit register. Up to now, single-shot readout in superconducting processors has been achieved only for phase qubits.[12,13] In a multiphase-qubit processor equipped with single-shot but destructive readout of each qubit, the Deutsch-Jozsa algorithm[9] was demonstrated in Ref. 12 with a success probability of order 0.7 in a single run, to be compared to 0.5 for a classical algorithm. Very recently a similar processor ran a compiled version of Shor's algorithm,[2] yielding prime factors of 15 with a 48% success rate.[14]

Since the Deutsch-Jozsa classification algorithm is not directly related to any practical situation, demonstrating quantum speed-up for more useful algorithms in an electrical processor designed along the blueprint of Fig. 1 is an important goal.[14] In this Rapid Communication, we report the operation of a two-transmon-qubit processor[15] that comes closer to the ideal scheme than those previously mentioned, and the single-shot run of the Grover search algorithm among four objects. Since, in this case, the algorithm ideally yields the answer after one algorithm step, its success probability after a single run provides a simple benchmark. We find that our processor yields the correct answer at each run, with a success probability that ranges between 0.52 and 0.67, whereas a single-step classical algorithm using a random query would yield the correct answer with probability 0.25.

The sample and the setup used for this experiment are the very same as those described and characterized in detail in Ref. 15. The sample fabrication and parameters are summarized in Secs. I and II of the Supplemental Material,[16] whereas the scheme of our processor and its mode of operation are recalled in Fig. 2: Two tunable transmon qubits coupled by a fixed capacitor are embedded in two identical control and readout subcircuits. The Hamiltonian of the two qubits {I,II} is $H/h = (-\nu_{\rm I}\sigma_z^{\rm I} - \nu_{\rm II}\sigma_z^{\rm II} + 2g\sigma_y^{\rm I}\sigma_y^{\rm II})/2$, where $\sigma_{x,y,z}$ are the Pauli operators, $\nu_{\rm I,II}$ are the qubit frequencies controlled by the flux applied to each transmon superconducting quantum intereference device (SQUID) loop with fast (0.5-GHz bandwidth) local current lines, and $g = 4.6$ MHz $\ll \nu_{\rm I,II}$ is the coupling frequency controlled by the coupling capacitance (see Sec. II of the Supplemental Material and Ref. 17). The achieved frequency control allows us to place the two transmons on resonance during times precise enough for performing the universal two-qubit gate $\sqrt{\rm iSWAP}$ (Ref. 15) and the exchange gate iSWAP used in this work. The qubit frequencies are tuned to different values for single-qubit manipulation, two-qubit gate operation, and readout (see Sec. III of the Supplemental Material[16]). The readout is independently and simultaneously performed for each qubit using the single-shot method of Ref. 18. It is based on the dynamical transition of a nonlinear resonator[19,20] that maps the quantum state of each transmon to the bifurcated or nonbifurcated state of its resonator, which

 

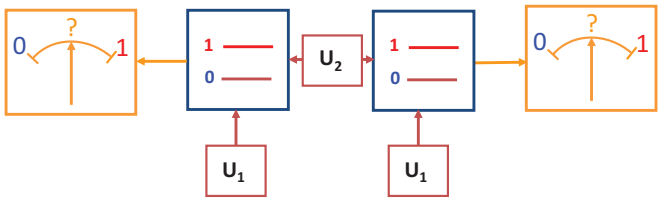


FIG. 1. (Color online) Schematic blueprint of a quantum processor based on quantum gates, represented here in the two-qubit case relevant for our experiment. A quantum processor consists of a qubit register that can perform any unitary evolution needed by an algorithm under the effect of a universal set of quantum gates (single-qubit gate $U_1$, two-qubit gate $U_2$). Ideally, all the qubits may be read projectively, and may be reset.

yields a binary outcome for each qubit. This readout method is potentially nondestructive, but its nondestructive character is presently limited by relaxation during the readout pulse. In order to further improve the readout fidelity, we resort to a shelving method that exploits the second excited state of the transmon. For this purpose, a microwave pulse that induces a transition from state $|1\rangle$ toward the second excited state $|2\rangle$ of the transmon is applied just before the readout pulse, as demonstrated in Ref. 18 (this variant does not alter the nondestructive aspect of the readout method since an extra pulse bringing state $|2\rangle$ back to state $|1\rangle$ could be applied after readout). Although the readout contrast achieved with this shelving method and with optimized microwave pulses reaches 0.88 and 0.89 for the two qubits, respectively, the values achieved at working points suitable for processor operation are lower and equal to 0.84 and 0.83. The sources of readout errors are discussed in Sec. IV of the Supplemental Material[16] and include a small readout crosstalk contribution. The overall readout fidelity is thus characterized by a $4 \times 4$ matrix $\mathcal{R}$, giving the readout outcome probabilities for each of the input states of the two-qubit register.

In order to characterize the evolution of this register during the algorithm, we determine its density matrix by state tomography. For this purpose, we measure the expectation values of the extended Pauli set of operators $\{\sigma_x I, \ldots, \sigma_z \sigma_z\}$ by applying the suitable rotations just before readout and by averaging typically $10^4$ times. Note that the readout errors are corrected by inverting the readout matrix $\mathcal{R}$ when determining the expectation value of the Pauli set, and thus do not contribute to tomography errors, as explained in Ref. 15. The density matrix $\rho$ is then taken as the acceptable positive-semidefinite matrix that, according to the Hilbert-Schmidt distance, is the closest to the possibly nonphysical one derived from the measurement set. In order to characterize the fidelity of the algorithm at all steps, we use the state fidelity $F = \langle\psi|\rho|\psi\rangle$, with $|\psi\rangle$ the ideal quantum state at the step considered; $F$ is in this case the probability for the qubit register to be in state $|\psi\rangle$.

The Grover search algorithm[1] consists of retrieving a particular basis state in a Hilbert space of size $N$ using a function able to discriminate it from the other ones. This function is used to build an oracle operator that tags the searched state. Starting from the superposition $|\phi\rangle$ of all register states, a unitary sequence that incorporates the oracle operator is repeated about $\sqrt{N}$ times, and eventually yields the

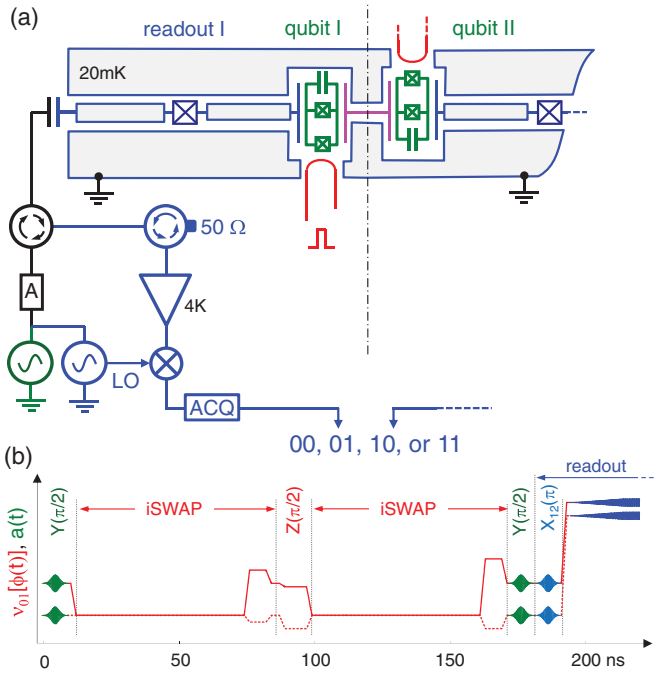


FIG. 2. (Color online) Electrical scheme of the two-qubit circuit operated and typical sequence during processor operation. (a) Two capacitively coupled transmon qubits have tunable frequencies controlled by the flux induced in their SQUID loop by a local current line. The coupling capacitance (center) yields a swapping evolution between the qubits when on resonance. Each transmon is embedded in a nonlinear resonator used for single-shot readout. Each reflected readout pulse is routed to a cryogenic amplifier through circulators, homodyned at room temperature, and acquired digitally, which yields a two-bit outcome. (b) Typical operation of the processor showing the resonant microwave pulses $a(t)$ applied to the qubits and to the readouts, on top of the dc pulses (polylines) that vary the transition frequencies of qubit I (solid) and II (dashed). With the qubits tuned at a first working point for single-qubit gates, resonant pulses are applied for performing $X$ and $Y$ rotations, as well as small flux pulses for $Z$ rotations; qubits are then moved to the interaction point for two-qubit gate operations. Such sequences can be combined as needed by the algorithm. Qubits are then moved to their initial working points for applying tomography pulses as well as a $|1\rangle \rightarrow |2\rangle$ pulse $X_{12}(\pi)$ to increase the fidelity of the forthcoming readout. Finally, they are moved to better readout points and read.

searched state with a high probability. The implementation of Grover's algorithm in a two-qubit Hilbert space often proceeds in a simpler way[21–26] since the result is obtained with certainty after a single algorithm step. The algorithm then consists of an encoding sequence depending on the searched state, followed by a universal decoding sequence that retrieves it. Grover's algorithm thus provides a simple benchmark for two-qubit processors. Its implementation with our quantum processor is shown in Fig. 3(a). First, the superposed state $|\phi\rangle$ is obtained by applying $\pi/2$ rotations around the $Y$ axis for the two qubits. The oracle operator $O_{uv}$ tagging the two-qubit state $|uv\rangle \equiv |u\rangle_{\mathrm{I}} \otimes |v\rangle_{\mathrm{II}}$ to be searched is then applied to state $|\phi\rangle$. Each $O_{uv}$ consists of an iSWAP gate followed by a $Z(\pm\pi/2)$ rotation on each qubit, with the four possible sign combinations $(-,-)$, $(+,-)$, $(-,+)$, and $(+,+)$ corresponding to $uv = 00$, 01, 10, and 11, respectively. In the algorithm we

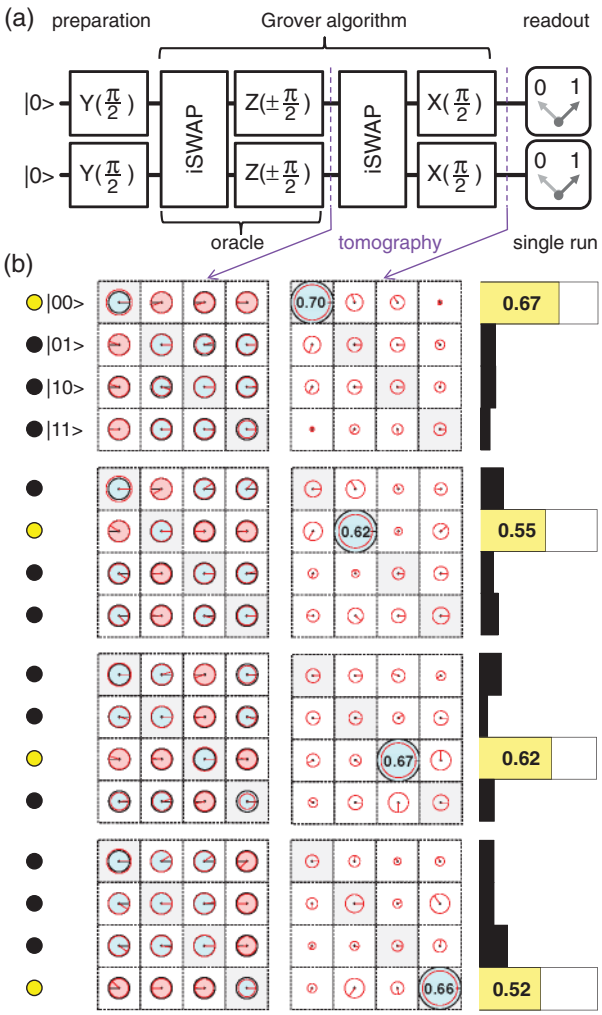


FIG. 3. (Color online) (a) Experimental sequence used for implementing the Grover search algorithm on four objects. First, $Y(\pi/2)$ rotations are applied to produce the superposition $|\phi\rangle = (1/2)\sum_{u,v}|uv\rangle$ of all basis states; then one of the four possible oracles (corresponding to the four sign combinations of the $Z$ rotations) is applied. The tagged state is then decoded in all cases using an iSWAP operation followed by $X(\pi/2)$ rotations. (b) State tomography at two steps of the algorithm ($\rho$ matrices) and success probability after a single run (histograms). The bright dots on the left-hand side mark the basis state tagged by each oracle operator used. The amplitude of each matrix element is represented by a disk [black for the ideal density matrix, red (gray) for the measured one] and its phase by an arrow (as well as a filling color for the ideal matrix). After applying the oracle, the information on the tagged state is encoded in the phase of six particular elements of $\rho$. After decoding, the tagged state should be the only matrix element present in $\rho$. The fidelity $F_{\text{final}}$ actually obtained is indicated in this element. The probability distribution of the single-run readout outcomes is shown on the right-hand side (bright box for the correct answer, solid dark boxes for the wrong ones).

use, the encoding is a phase encoding as in Ref. 10. When applied to $|\phi\rangle$, each oracle operator inverts the sign of the component corresponding to the state it tags, respectively, to the other ones. The density matrix, after applying the oracle, ideally takes a simple form: The amplitude of all coefficients is 1/4, and the phase of an element $\rho_{rs}$ is $\varphi_{rs} = \pi(\delta_{rt} + \delta_{st})$, where $t$ corresponds to the state tagged by the oracle operator. The state tomography performed after applying the oracle, shown in Fig. 3(b), is in good agreement with this prediction. More quantitatively, we find that after having applied the oracle operator, the intermediate fidelity is $F_{\text{int}} = 0.87$, 0.80, 0.84, and 0.82, respectively. The last part of the algorithm consists in transforming the obtained state in the searched state irrespectively of it, or equivalently to transform the phase information distributed over the elements of the density matrix in a weight information with the whole weight on the searched state. This operation is readily performed by applying an iSWAP gate followed by $X(\pi/2)$ rotations for both qubits. We find that the fidelity of the density matrix at the end of the algorithm is $F_{\text{final}} = 0.70$, 0.62, 0.67, and 0.66, respectively. We explain both $F_{\text{int}}$ and $F_{\text{final}}$ by gate errors at a 2% level, by errors in the tomography pulses at a 2% level, as well as by decoherence during the whole experimental sequence [at the coupling point, relaxation times are $T_1^{\text{I}} \simeq 450$ ns and $T_1^{\text{II}} \simeq 500$ ns, and the effective dephasing times $T_\varphi^{\text{I}} \simeq T_\varphi^{\text{II}} \simeq 2\ \mu$s (Ref. 15)].

We now consider the success probability obtained after a single run (with no tomography pulses), which probes the quantum speed-up actually achieved by the processor. We find (see Fig. 3) that our processor does yield the correct answer with a success probability $P_{\text{S}} = 0.67$, 0.55, 0.62, and 0.52 for the four basis states, which is smaller than the density matrix fidelity $F_{\text{final}}$. One notices that the difference between $F_{\text{final}}$ and $P_{\text{S}}$, mostly due to readout errors, slightly depends on the searched state: The larger the energy of the searched state, the larger is the difference. This dependence is well explained by the effect of relaxation during the readout pulse, which is the main error source at readout, the second one being readout crosstalk. One also notices that the outcome errors are distributed over all the wrong answers. To summarize, the errors of our implementation of Grover's algorithm originate both from small unitary errors accumulated during the algorithm, and from decoherence during the whole sequence, in particular, during the final readout.

We finally discuss the significance of the obtained results in terms of quantum information processing. The achieved success probability is smaller than the theoretically achievable value 1, but nevertheless it is sizably larger than the value of 0.25 obtained by running once the classical algorithm that consists in making a random trial. From the point of view of a user who has to find out which unknown oracle has been given to him, the fidelity of the algorithm outcome is $f_{ab} = 0.57$, 0.63, 0.57, and 0.59 for the 00, 01, 10, and 11 outcomes, respectively, as explained in Sec. V of the Supplemental Material.[16] Despite the presence of errors, this result demonstrates the quantum speed-up for Grover's algorithm when searching in a Hilbert space with a small size $N = 4$.

In conclusion, we have demonstrated the operation of the Grover search algorithm in a superconducting two-qubit processor with a single-shot nondestructive readout. This result indicates that the quantum speed-up expected from quantum algorithms is within reach of superconducting quantum bit processors. Demonstrating the $\sqrt{N}$ speed-up for Grover's algorithm in larger Hilbert spaces requires a qubit architecture

more scalable than the present one, which presently is a major challenge in the field.

We gratefully acknowledge discussions with M. Devoret, D. DiVicenzo, L. DiCarlo, and within the Quantronics group, technical support from P. Orfila, P. Senat, and J. C. Tack, as well as financial support from the European research contract SOLID, from ANR Masquelspec and C'Nano, and from the German Ministry of Education and Research.

[1] L. K. Grover, in *Proceedings of the 28th Annual ACM Symposium on the Theory of Computing*, edited by G. L. Miller (ACM, New York, 1996), p. 212; Am. J. Phys. **69**, 769 (2001).

[2] P. W. Shor, *Proceedings of the 35th Annual Symposium on Foundations of Computer Science* (IEEE, Los Alamitos, CA, 1994); SIAM J. Comput. **26**, 1484 (1997).

[3] M. A. Nielsen and I. L. Chuang, *Quantum Computation and Quantum Information* (Cambridge University Press, Cambridge, UK, 2000).

[4] T. D. Ladd, F. Jelezko, R. Laflamme, Y. Nakamura, C. Monroe, and J. L. O'Brien, Nature (London) **464**, 45 (2010).

[5] D. P. DiVincenzo, Fortschr. Phys. **48**, 771 (2000).

[6] J. Koch, T. M. Yu, J. Gambetta, A. A. Houck, D. I. Schuster, J. Majer, A. Blais, M. H. Devoret, S. M. Girvin, and R. J. Schoelkopf, Phys. Rev. A **76**, 042319 (2007).

[7] J. A. Schreier, A. A. Houck, J. Koch, D. I. Schuster, B. R. Johnson, J. M. Chow, J. M. Gambetta, J. Majer, L. Frunzio, M. H. Devoret, S. M. Girvin, and R. J. Schoelkopf, Phys. Rev. B **77**, 180502 (2008).

[8] Y. Nakamura, Yu. A. Pashkin, and J. S. Tsai1, Nature (London) **398**, 786 (1999).

[9] D. Deutsch and R. Jozsa, Proc. R. Soc. London A**439**, 553 (1992).

[10] L. DiCarlo, J. M. Chow, J. M. Gambetta, L. S. Bishop, B. R. Johnson, D. I. Schuster, J. Majer, A. Blais, L. Frunzio, S. M. Girvin, and R. J. Schoelkopf, Nature (London) **460**, 240 (2009).

[11] M. D. Reed, L. DiCarlo, S. E. Nigg, L. Sun, L. Frunzio, S. M. Girvin, and R. J. Schoelkopf, Nature (London) **482**, 382 (2012).

[12] T. Yamamoto, M. Neeley, E. Lucero, R. C. Bialczak, J. Kelly, M. Lenander, M. Mariantoni, A. D. O'Connell, D. Sank, H. Wang, M. Weides, J. Wenner, Y. Yin, A. N. Cleland, and J. M. Martinis, Phys. Rev. B **82**, 184515 (2010).

[13] M. Mariantoni, H. Wang, T. Yamamoto, M. Neeley, R. C. Bialczak, Y. Chen, M. Lenander, E. Lucero, A. D. O'Connell, D. Sank, M. Weides, J. Wenner, Y. Yin, J. Zhao, A. N. Korotkov, A. N. Cleland, and J. M. Martinis, Science **334**, 6052 (2011).

[14] E. Lucero, R. Barends, Y. Chen, J. Kelly, M. Mariantoni, A. Megrant, P. O'Malley, D. Sank, A. Vainsencher, J. Wenner, T. White, Y. Yin, A. N. Cleland, and J. M. Martinis, e-print arXiv:1202.5707.

[15] A. Dewes, F. R. Ong, V. Schmitt, R. Lauro, N. Boulant, P. Bertet, D. Vion, and D. Esteve, Phys. Rev. Lett. **108**, 057002 (2012).

[16] See Supplemental Material at http://link.aps.org/supplemental/10.1103/PhysRevB.85.140503 for technical information about the sample preparation (I), sample parameters (II), and experimental setup (III), and for the detailed analysis of readout errors (IV) and algorithm fidelity (V).

[17] F. R. Ong, M. Boissonneault, F. Mallet, A. Palacios-Laloy, A. Dewes, A. C. Doherty, A. Blais, P. Bertet, D. Vion, and D. Esteve, Phys. Rev. Lett. **106**, 167002 (2011).

[18] F. Mallet, Florian R. Ong, A. Palacios-Laloy, F. Nguyen, P. Bertet, D. Vion, and D. Esteve, Nat. Phys. **5**, 791 (2009).

[19] I. Siddiqi, R. Vijay, F. Pierre, C. M. Wilson, M. Metcalfe, C. Rigetti, L. Frunzio, and M. H. Devoret, Phys. Rev. Lett. **93**, 207002 (2004).

[20] M. B. Metcalfe, E. Boaknin, V. Manucharyan, R. Vijay, I. Siddiqi, C. Rigetti, L. Frunzio, R. J. Schoelkopf, and M. H. Devoret, Phys. Rev. B **76**, 174516 (2007).

[21] J. A. Jones, M. Mosca, and R. H. Hansen, Nature (London) **393**, 344 (1998).

[22] I. L. Chuang, N. Gershenfeld, and M. Kubinec, Phys. Rev. Lett. **80**, 3408 (1998).

[23] K. A. Brickman, P. C. Haljan, P. J. Lee, M. Acton, L. Deslauriers, and C. Monroe, Phys. Rev. A **72**, 050306 (2005).

[24] N. Bhattacharya, H. B. van Linden van den Heuvell, and R. J. C. Spreeuw, Phys. Rev. Lett. **88**, 137901 (2002).

[25] P. Walther, K. J. Resch, T. Rudolph, E. Schenck, H. Weinfurter, V. Vedral, M. Aspelmeyer, and A. Zeilinger, Nature (London) **434**, 169 (2005).

[26] J. Ahn, T. C. Weinacht, and P. H. Bucksbaum, Science **287**, 463 (2000).